Rapid formation of large dust grains in the luminous supernova SN 2010jl

Christa Gall[1,2,3], Jens Hjorth[2], Darach Watson[2], Eli Dwek[3], Justyn R. Maund[4,2], Ori Fox[5], Giorgos Leloudas[6,2], Daniele Malesani[2] & Avril C. Day-Jones[7]

[1]*Department of Physics and Astronomy, Aarhus University, Ny Munkegade 120, DK-8000 Aarhus C, Denmark*

[2]*Dark Cosmology Centre, Niels Bohr Institute, University of Copenhagen, Juliane Maries Vej 30, DK-2100 Copenhagen Ø, Denmark*

[3]*Observational Cosmology Lab, Code 665, NASA Goddard Space Flight Center, Greenbelt, MD 20771, USA*

[4]*Astrophysics Research Centre School of Mathematics and Physics Queen's University Belfast Belfast BT7 1NN, UK*

[5]*Department of Astronomy, University of California, Berkeley, CA 94720-3411, USA*

[6]*The Oskar Klein Centre, Department of Physics, Stockholm University, Albanova University Centre, 10691, Stockholm, Sweden*

[7]*Departamento de Astronomia, Universidad de Chile, Camino del Observatorio 1515, Santiago, Chile*

The origin of dust in galaxies is still a mystery (1, 2, 3, 4). The majority of the refractory elements are produced in supernova explosions but it is unclear how and where dust grains condense and grow, and how they avoid destruction in the harsh environments of star-forming

galaxies. The recent detection of 0.1–0.5 solar masses of dust in nearby supernova remnants (5, 6, 7) suggests *in situ* dust formation, while other observations reveal very little dust in supernovae the first few years after explosion (1, 8, 9, 10). Observations of the bright SN 2010jl have been interpreted as pre-existing dust (11), dust formation (12, 13) or no dust at all (14). Here we report the rapid (40–240 days) formation of dust in its dense circumstellar medium. The wavelength dependent extinction of this dust reveals the presence of very large (> 1 μm) grains, which are resistant to destructive processes (15). At later times (500–900 days), the near-IR thermal emission shows an accelerated growth in dust mass, marking the transition of the supernova from a circumstellar- to an ejecta-dominated source of dust. This provides the link between the early and late dust mass evolution in supernovae with dense circumstellar media.

We observed the bright ($V \sim 14$) and luminous ($M_V \sim -20$) Type IIn SN 2010jl (16) with the VLT/X-shooter spectrograph covering the wide wavelength range 0.3–2.5 μm. Peak brightness occurred on 2010 Oct 18.6 UT, and observations were made at 9 early epochs and at one late epoch, 26–239 and 868 days past peak, respectively (Methods, Extended Data Table 1, Extended Data Figures 1–5). Figure 1 shows the intermediate-width components of the hydrogen emission lines of Hγ at λ4340.472 and Pβ at λ12818.072 and of the oxygen ejecta emission lines [O I] $\lambda\lambda$6300.304, 6363.776 (rest frame). The emission profiles change with time, exhibiting a substantial depression of the red wings and a corresponding blueshift of the centroids of the lines (Extended Data Figure 6) due to preferential extinction of the emission from the receding material on the far side of the supernova (12, 17, 18). The effect is less pronounced at longer wavelengths, as expected if the attenuation of the lines is due to dust extinction, and rules out that the blueshifts are due to electron scattering (14) (Supplementary Information). The early epoch hydrogen lines have a Lorentzian half width at half maximum (HWHM) in the range 1,000–2,000 km s $^{-1}$. The middle and right panels of Figure 1 show that the line profiles at the late epoch are narrower (HWHM $\sim$ 800 ± 100 km s^{-1}) and also exhibit blueshifts of the oxygen lines, which indicates that ejecta material is involved in the dust formation at this stage.

Figure 2 shows the temporal evolution of the inferred extinction, A_λ, as derived from the attenuation of emission lines in the early spectra. The extinction has been calculated from the ratios of the integrated line profiles at each epoch. We assume that the first epoch at 26 days past peak is nearly unextinguished and use it as a reference. The monotonic increase of the extinction as a function of time indicates continuous formation of dust. The extinction at 239 days is $A_V \sim 0.6$ mag. Interestingly, the shape of the normalized extinction curve shows no substantial variation with time. Scaling and combining the data from the eight individual early epochs allows us to produce the first directly measured, robust extinction curve for a supernova. The extinction curve is shallow, with $R_V = A_V/E(B-V) \approx 6.4$, and can be represented by a mix of grey-extinction dust grains (A_λ = constant) and either standard Small Magellanic Cloud (SMC) or Milky Way (MW) extinction grains (19). The extinction contribution of the grey dust is 40 % in the V band. We fit several dust models to the extinction curve using amorphous carbon dust characterized by a power-law grain size distribution (20) with slope α, and minimum and maximum grain radii ($a_{\mathrm{min}} < a_{\mathrm{max}}$) in the interval [0.001, 5.0] μm.

Figure 3 shows the resulting confidence interval for the two parameters $a_{\rm max}$ and α around the best fit values of $a_{\rm min} = 0.001\ \mu$m, $a_{\rm max} = 4.2\ \mu$m and $\alpha = 3.6$. It is evident that only size distributions extending to grain radii that are significantly larger than that of MW interstellar medium (21, 22) dust ($\gtrsim 0.25\ \mu$m) can reproduce the supernova extinction curve (Figure 2). The 2 σ lower limit on the maximum grain size is $a_{\rm max} > 0.7\ \mu$m. We cannot perform a similar analysis of the late epoch because the intrinsic line profile at this epoch is unknown and likely highly affected by extinction (13). However, we note that the blueshift velocities change only marginally with wavelength (Extended Data Figure 6), suggestive of large grains also at this epoch.

Figure 4 illustrates the continuous build-up of dust as a function of time. The increasing attenuation of the lines is accompanied by increasing emission in the near-infrared (NIR) spectra, from a slight excess over a supernova blackbody fit at early times to total dominance at the late epoch. We fitted the spectra with black bodies which for the NIR excess yield a constant black-body radius of $(1.0 \pm 0.2) \times 10^{16}$ cm at the early epochs, and a temperature that declines from $\sim$ 2,300 K to $\sim$ 1,600 K from day 26 onwards. At the late epoch, we obtain a black-body radius of $(5.7 \pm 0.2) \times 10^{16}$ cm and a temperature of $\sim$ 1,100 K. The high temperatures detected at the early epochs suggest that the NIR excess is due to thermal emission from carbonaceous dust, rather than silicate dust, which has a lower condensation temperature of $\sim 1,500$ K (1). The high temperatures rule out suggestions that the NIR emission is due to pre-existing dust or a dust echo (11) (Extended Data Figures 7, 8, Supplementary Information). Fitting the NIR excess with a modified black body, assuming the grain composition found in our analysis of the extinction curve (Figure 3), gives a dust temperature similar to the black-body temperature, which is at all epochs (and considered dust compositions) larger than 1,000 K. The dust masses inferred from the extinction and NIR emission agree very well. The inferred amount of dust at the late epoch (868 days) is $\sim 2.5 \times 10^{-3}$ $M_\odot$ if composed of carbon, but could be up to an order of magnitude larger for silicates (Methods). Our results indicate accelerated dust formation after several hundred days. SN 2010jl will contain a dust mass of $\sim$ 0.5 $M_\odot$ similar to that observed in SN 1987A (5, 6), by day $\sim$ 8000, if the dust production continues to follow the trend depicted in Figure 4.

The most obvious location for early dust formation is in a cool, dense shell behind the supernova shock (18, 23), which sweeps up material as it propagates through the dense circumstellar shell surrounding SN 2010jl (24) (Supplementary Information). Dust formation in the ejecta is impossible at this stage because the temperature is too high. The postshock gas cools and gets compressed to the low temperatures and high densities necessary for dust formation and gives rise to the observed intermediate width emission lines. By the time of our first observation 26 days past peak, the supernova blast wave encounters the dense circumstellar shell at a radius of $\sim 2.0 \times 10^{16}$ cm for a blast wave velocity of $\sim 3.5 \times 10^4$ km s^{-1}. As indicated by the blueshifts of the ejecta metal lines (Figure 1), the accelerated dust formation occurring at later times (Figure 4) and at larger radius is possibly facilitated by the bulk ejecta material, which travels on average at a velocity of $\sim 7,500$ km s^{-1} at early epochs (Extended Data Figure 4).

Our detection of large grains soon after the supernova explosion suggests a remarkably rapid and efficient mechanism for dust nucleation and growth. The underlying physics is poorly understood but may involve a two-stage process governed by early dust formation in a cool, dense shell, followed by accelerated dust formation involving ejecta material. For Type IIP supernovae, the growth of dust grains can be sustained up to 5 years past explosion (25). The dense CSM around Type IIn supernovae may provide conditions to facilitate dust growth beyond that. The process appears generic, in that other Type IIn supernovae like SN 1995N, SN 1998S, SN 2005ip, and SN 2006jd exhibited similar observed NIR properties (8, 10, 26, 27) and growing dust masses, consistent with the trend revealed here for SN 2010jl (Figure 4). Moreover, it establishes a link between the early small dust masses inferred in supernovae (1, 8, 10) and the large dust masses found in a few supernova remnants (1, 5, 7). Large grains ($0.1 \leq a_{\mathrm{max}} \lesssim 4.0\ \mu$m), provide an effective way to counter destructive processes in the interstellar medium (28). Indeed, large grains from the interstellar medium have been detected in the Solar System (29). Simulations indicate that grains larger than $\sim 0.1\ \mu$m will survive reverse shock interactions with only a low fraction being sputtered to smaller radii (15). For a grain size distribution of $a_{\mathrm{min}} = 0.001\ \mu$m, $a_{\mathrm{max}} = 4.2\ \mu$m and $\alpha = 3.6$ (Figures 2 and 3), the mass fraction of grains above $0.1\ \mu$m is ~ 80 %, i.e., the majority of the produced dust mass can be retained.

Methods summary

We obtained optical and near-infrared medium-resolution spectroscopy with the ESO VLT/X-shooter instrument of the bright Type IIn supernova SN 2010jl at 9 epochs between 2010 November 13.4 UT and 2011 June 15.0 UT. The continuum emission of the spectra was fit with a combination of black-body, modified black-body and host galaxy models, allowing us to quantify the temporal progression of the temperature and radius of the photosphere as well as the temperature and characteristics of the forming dust, which causes conspicuous excess near-infrared emission. We analysed the profiles of the most prominent hydrogen, helium and oxygen emission lines. From Lorentzian profile fits, which are good representations of the emission lines, we measured the blueshifts of the peaks and the half widths at half maximum of the lines, and derived the wavelength dependent attenuation properties of the forming dust at each epoch. The uncertainties were obtained using Monte Carlo calculations by varying the Lorentzian profile parameters. We generated synthetic UBVRIJHK lighcurves and calculated the energy output of the supernova. This, together with calculated dust vaporization radii, temperatures of the dust grains at different distances from the supernova, and the radius evolution of the forward shock, were used to constrain the location of the forming dust. Different dust models, characterised by either single grain sizes or a power-law grain size distribution function and either amorphous carbon or silicates, were fitted to the extinction curves and the near-infrared excess emission. From these fits, we derived the temporal progression of the dust mass of the forming dust at each observed epoch.

1. Gall, C., Hjorth, J. & Andersen, A. C. Production of dust by massive stars at high redshift. *Astron. Astrophys. Rev.* **19**, 43 (2011). `1108.0403`.
2. Matsuura, M. *et al.* The global gas and dust budget of the Large Magellanic Cloud: AGB stars and supernovae, and the impact on the ISM evolution. *Mon. Not. R. Astron. Soc.* **396**, 918–934 (2009). `0903.1123`.
3. Draine, B. T. Interstellar Dust Models and Evolutionary Implications. In Henning, T., Grün, E. & Steinacker, J. (eds.) *Cosmic Dust - Near and Far*, vol. 414 of *Astronomical Society of the Pacific Conference Series*, 453 (2009). `0903.1658`.
4. Dunne, L. *et al.* Herschel-ATLAS: rapid evolution of dust in galaxies over the last 5 billion years. *Mon. Not. R. Astron. Soc.* **417**, 1510–1533 (2011). `1012.5186`.
5. Matsuura, M. *et al.* Herschel Detects a Massive Dust Reservoir in Supernova 1987A. *Science* **333**, 1258– (2011). `1107.1477`.
6. Indebetouw, R. *et al.* Dust Production and Particle Acceleration in Supernova 1987A Revealed with ALMA. *Astrophys. J. Lett.* **782**, L2 (2014). `1312.4086`.
7. Gomez, H. L. *et al.* A Cool Dust Factory in the Crab Nebula: A Herschel Study of the Filaments. *Astrophys. J.* **760**, 96 (2012). `1209.5677`.
8. Pozzo, M. *et al.* On the source of the late-time infrared luminosity of SN 1998S and other Type II supernovae. *Mon. Not. R. Astron. Soc.* **352**, 457–477 (2004). `astro-ph/0404533`.

9. Otsuka, M. *et al.* Late-time Light Curves of Type II Supernovae: Physical Properties of Supernovae and Their Environment. *Astrophys. J.* **744**, 26 (2012). `1111.5041`.

10. Stritzinger, M. *et al.* Multi-wavelength Observations of the Enduring Type IIn Supernovae 2005ip and 2006jd. *Astrophys. J.* **756**, 173 (2012). `1206.5575`.

11. Andrews, J. E. *et al.* Evidence for Pre-existing Dust in the Bright Type IIn SN 2010jl. *Astron. J.* **142**, 45 (2011). `1106.0537`.

12. Smith, N. *et al.* Systematic Blueshift of Line Profiles in the Type IIn Supernova 2010jl: Evidence for Post-shock Dust Formation? *Astron. J.* **143**, 17 (2012). `1108.2869`.

13. Maeda, K. *et al.* Properties of Newly Formed Dust Grains in the Luminous Type IIn Supernova 2010jl. *Astrophys. J.* **776**, 5 (2013). `1308.0406`.

14. Zhang, T. *et al.* Type IIn Supernova SN 2010jl: Optical Observations for over 500 Days after Explosion. *Astron. J.* **144**, 131 (2012). `1208.6078`.

15. Silvia, D. W., Smith, B. D. & Shull, J. M. Numerical Simulations of Supernova Dust Destruction. I. Cloud-crushing and Post-processed Grain Sputtering. *Astrophys. J.* **715**, 1575–1590 (2010). `1001.4793`.

16. Newton, J. & Puckett, T. Possible Supernova in UGC 5189A. *Central Bureau Electronic Telegrams* **2532**, 1 (2010).

17. Lucy, L. B., Danziger, I. J., Gouiffes, C. & Bouchet, P. Dust Condensation in the Ejecta of SN 1987 A. In Tenorio-Tagle, G., Moles, M. & Melnick, J. (eds.) *IAU Colloq. 120: Structure and*

Dynamics of the Interstellar Medium, vol. 350 of *Lecture Notes in Physics, Berlin Springer Verlag*, 164 (1989).

18. Smith, N., Foley, R. J. & Filippenko, A. V. Dust Formation and He II λ4686 Emission in the Dense Shell of the Peculiar Type Ib Supernova 2006jc. *Astrophys. J.* **680**, 568–579 (2008). `0704.2249`.

19. Gordon, K. D., Clayton, G. C., Misselt, K. A., Landolt, A. U. & Wolff, M. J. A Quantitative Comparison of the Small Magellanic Cloud, Large Magellanic Cloud, and Milky Way Ultraviolet to Near-Infrared Extinction Curves. *Astrophys. J.* **594**, 279–293 (2003). `astro-ph/0305257`.

20. Mathis, J. S., Rumpl, W. & Nordsieck, K. H. The size distribution of interstellar grains. *Astrophys. J.* **217**, 425–433 (1977).

21. Zubko, V., Dwek, E. & Arendt, R. G. Interstellar Dust Models Consistent with Extinction, Emission, and Abundance Constraints. *Astrophys. J. Suppl.* **152**, 211–249 (2004). `astro-ph/0312641`.

22. Brandt, T. D. & Draine, B. T. The Spectrum of the Diffuse Galactic Light: The Milky Way in Scattered Light. *Astrophys. J.* **744**, 129 (2012). `1109.4175`.

23. Fox, O. *et al.* Near-Infrared Photometry of the Type IIn SN 2005ip: The Case for Dust Condensation. *Astrophys. J.* **691**, 650–660 (2009). `0807.3555`.

24. Ofek, E. O. *et al.* SN 2010jl: Optical to Hard X-Ray Observations Reveal an Explosion Embedded in a Ten Solar Mass Cocoon. *Astrophys. J.* **781**, 42 (2014). `1307.2247`.

25. Sarangi, A. & Cherchneff, I. The Chemically Controlled Synthesis of Dust in Type II-P Supernovae. *Astrophys. J.* **776**, 107 (2013). `1309.5887`.

26. Mauerhan, J. & Smith, N. Supernova 1998S at 14 years postmortem: continuing circumstellar interaction and dust formation. *Mon. Not. R. Astron. Soc.* **424**, 2659–2666 (2012). `1204.1610`.

27. Van Dyk, S. D. Late-time Dust Emission from the Type IIn Supernova 1995N. *Astron. J.* **145**, 118 (2013). `1305.0028`.

28. Jones, A. P. & Nuth, J. A. Dust destruction in the ISM: a re-evaluation of dust lifetimes. *Astron. Astrophys.* **530**, A44 (2011).

29. Frisch, P. C. *et al.* Dust in the Local Interstellar Wind. *Astrophys. J.* **525**, 492–516 (1999). `astro-ph/9905108`.

30. Gallagher, J. S. *et al.* Optical and Infrared Analysis of Type II SN 2006bc. *Astrophys. J.* **753**, 109 (2012). `1205.5517`.

Supplementary Information

Is available in the online version of the paper.

Acknowledgments

We thank Lise Christensen and Teddy Frederiksen for advice on data reduction with the X-shooter pipeline and Maximilian Stritzinger and Rick Arendt for discussions. This investigation is based on observations made with ESO Telescopes at the La Silla Paranal Observatory under programme IDs 084.C-0315(D) and 087.C-0456(A). C.G. was supported from the NASA Postdoctoral Program (NPP) and acknowledges funding provided by the Danish Agency for Science and Technology and Innovation. G.L. is supported by the Swedish Research Council through grant No. 623-2011-7117. A.C.D.J. is supported by the Proyecto Basal PB06 (CATA), and partially supported by the Joint Committee ESO-Government Chile. The Dark Cosmology Centre is funded by the Danish National Research Foundation.

Author contributions

C.G. and J.H. conducted the observational campaign, reduced and analysed the data and wrote the manuscript. D.W. was the P.I. of the observing programs and assisted in writing the manuscript. E.D. performed calculations of vaporization radii and assisted in writing the manuscript. O.F. and G.L. assisted in data analysis. J.R.M. helped with the interpretation of the spectra and line profiles. D.M. and D.W. assisted with observations. A.C.D.J. conducted the observation of the epoch 2 spectrum. All authors were engaged in discussions and provided comments on the manuscript.

Author information

Reprints and permissions information is available at www.nature.com/reprints. The authors declare no competing financial interests. Readers are welcome to comment on the online version of the paper. Correspondence and requests for materials should be addressed to C.G. (cgall@phys.au.dk).

Figure 1 | Evolution of the hydrogen and oxygen line profiles in the spectrum of SN 2010jl. Line profiles for **a,** Hγ λ4340.472 and **b,** Pβ λ12818.072 for epochs from 26 to 239 days and **c,** Hγ and Pβ at 868 days. **d,** The [O I] $\lambda\lambda$6300.304, 6363.776 doublet (zero velocity set at λ6300.304), and **e,** the [O I] λ11297.68 line. The dashed-dotted lines in all panels denote zero velocity, at redshift $z = 0.01058$, as determined from narrow emission lines in the spectrum.

Figure 2 | Supernova dust extinction curves. a, The evolution of the extinction, A_λ, of the hydrogen lines (open circles with standard deviations; Methods). The solid lines represent the (linearly interpolated) extinction curves. **b,** The grey-shaded area represents the range of extinction curves relative to A_V (filled triangles with error bars). Grey curves are the SMC and MW extinction curves, while the red curves include a grey component (Methods). **c,** Fits to the optical depth within the 1, 2 and 3 σ (68.3, 95.4 and 99.7 %) confidence interval (Methods). Dashed and solid curves are models with 'best fitting' and MW parameters, respectively.

Figure 3 | Maximum grain size and slope of the grain size distribution. Confidence contours, as constrained by the normalized optical depth $\tau(\lambda)$ (see Figure 2). The most favorable power-law models lie within a parameter range for α between $\sim$ 3.4 and 3.7 and require large grains of $a_{\mathrm{max}} \gtrsim 1.3\,\mu$m ($1\sigma$). The confidence limits are as in Figure 2. Even at the 3σ confidence limit the maximum grain size is larger ($a_{\mathrm{max}} \gtrsim 0.5\,\mu$m) than MW maximum grain sizes for a power law model ($a_{\mathrm{max}} \approx 0.25\,\mu$m) (20) or more sophisticated models (21, 22).

Figure 4 | Temporal evolution of the dust mass. Carbon dust masses and standard deviation derived from the extinction (green band) and the NIR emission (red bars and band; Methods) including a literature data point at 553 days (13). The light grey shaded area illustrates the evolution of the early ($M_\mathrm{d} \propto t^{0.8}$ at $t < 250$ days) and late ($M_\mathrm{d} \propto t^{2.4}$ at $t > 250$ days) stages of dust formation when SN 2010jl switches from circumstellar to ejecta dust formation. The grey and blue symbols correspond to literature data for SN 2005ip (triangles), SN 2006jd (dots), and other supernovae (bars) (1, 5, 6, 9, 10, 27, 30). The length of the symbols for SN 1995N and SN1987A correspond to the quoted dust mass range. For other supernova the standard deviation is either smaller than the size of the symbols or have not been reported.

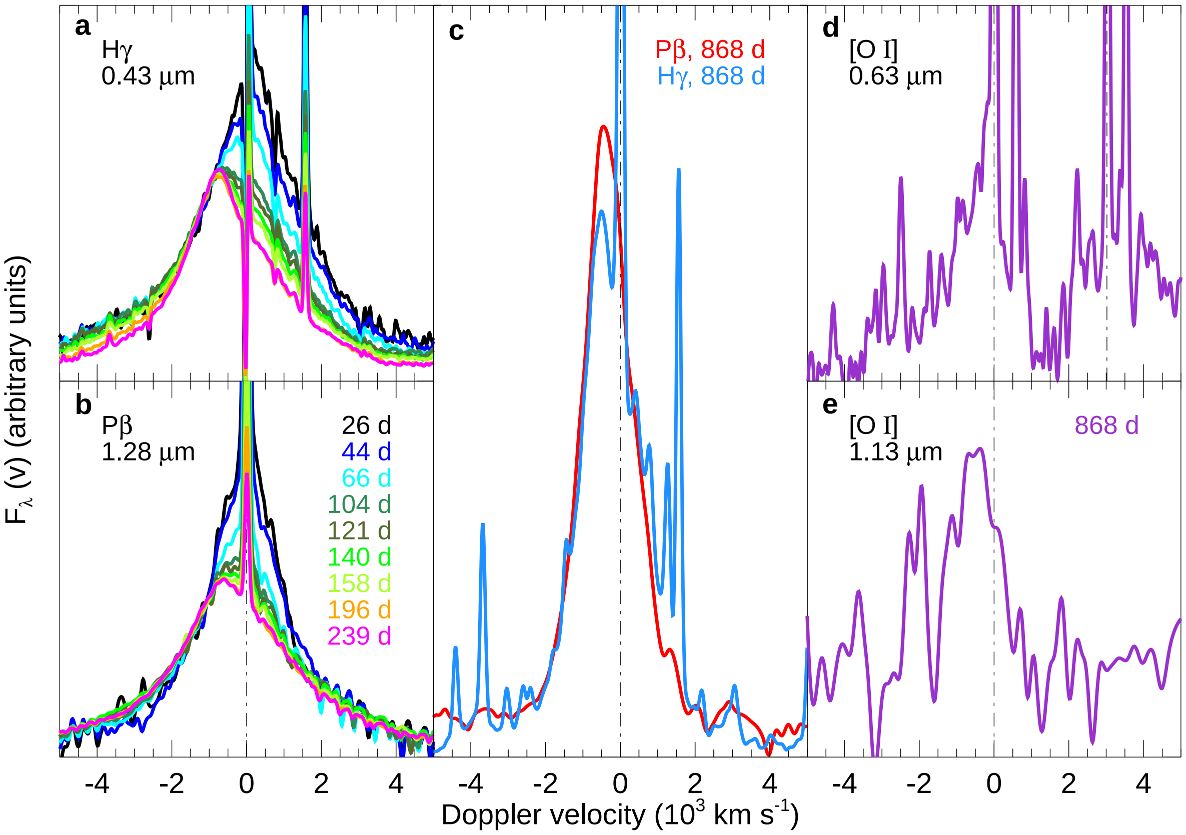
a
Hγ
0.43 μm
b
Pβ
1.28 μm
26 d
44 d
66 d
104 d
121 d
140 d
158 d
196 d
239 d
c
Pβ, 868 d
Hγ, 868 d
d
[O I]
0.63 μm
e
[O I]
1.13 μm
868 d
-4
-2
0
2
4
Doppler velocity (10^3 km s^{-1})
F$_λ$ (v) (arbitrary units)

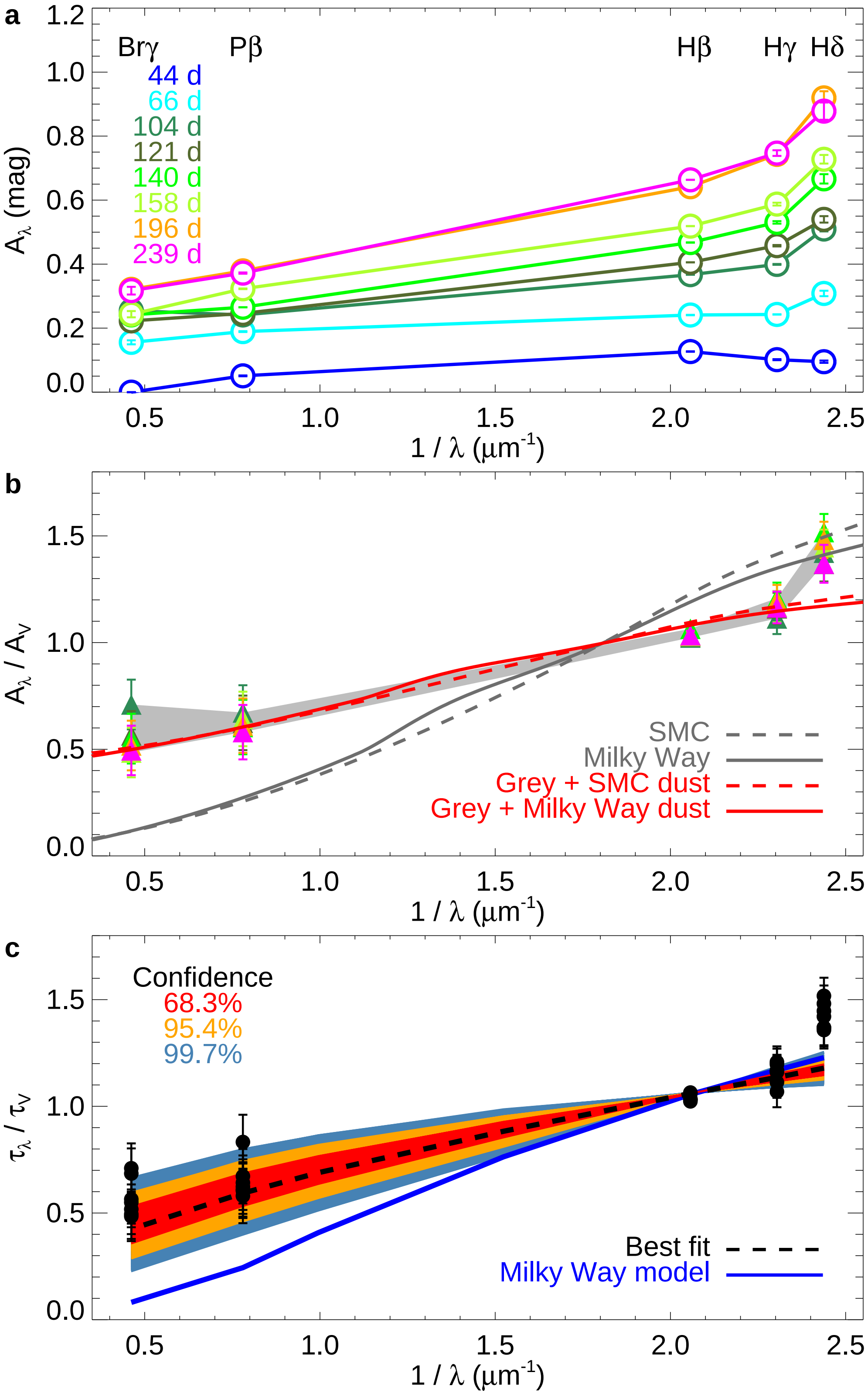
a
Brγ
Pβ
Hβ
Hγ
Hδ
44 d
66 d
104 d
121 d
140 d
158 d
196 d
239 d
A_λ (mag)
1.2
1.0
0.8
0.6
0.4
0.2
0.0
0.5
1.0
1.5
2.0
2.5
1 / λ (μm^{-1})
b
A_λ / A_V
1.5
1.0
0.5
0.0
SMC
Milky Way
Grey + SMC dust
Grey + Milky Way dust
0.5
1.0
1.5
2.0
2.5
1 / λ (μm^{-1})
c
Confidence
68.3%
95.4%
99.7%
τ_λ / τ_V
1.5
1.0
0.5
0.0
Best fit
Milky Way model
0.5
1.0
1.5
2.0
2.5
1 / λ (μm^{-1})

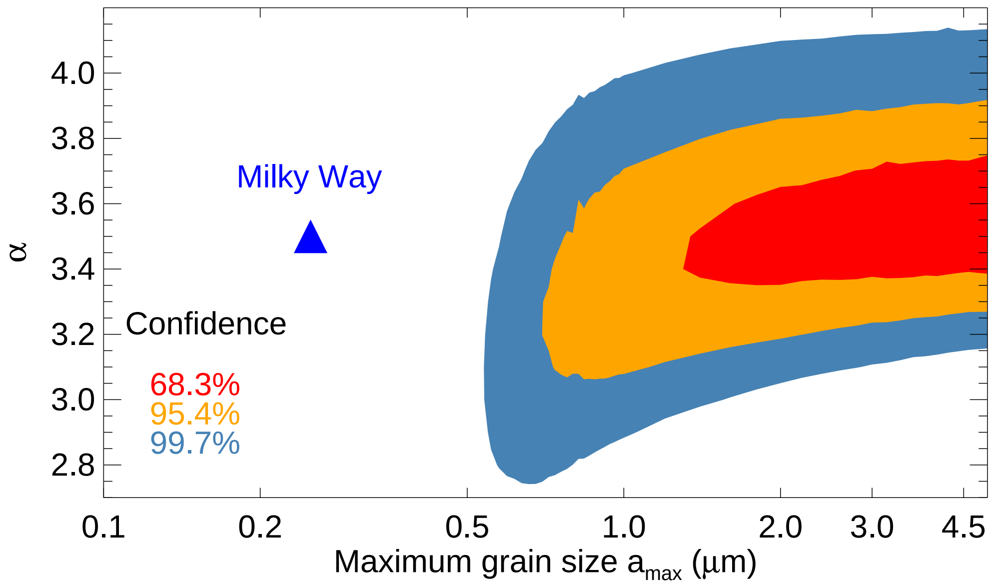
α
4.0
3.8
3.6
3.4
3.2
3.0
2.8
Milky Way
Confidence
68.3%
95.4%
99.7%
0.1
0.2
0.5
1.0
2.0
3.0
4.5
Maximum grain size a_{max} (μm)

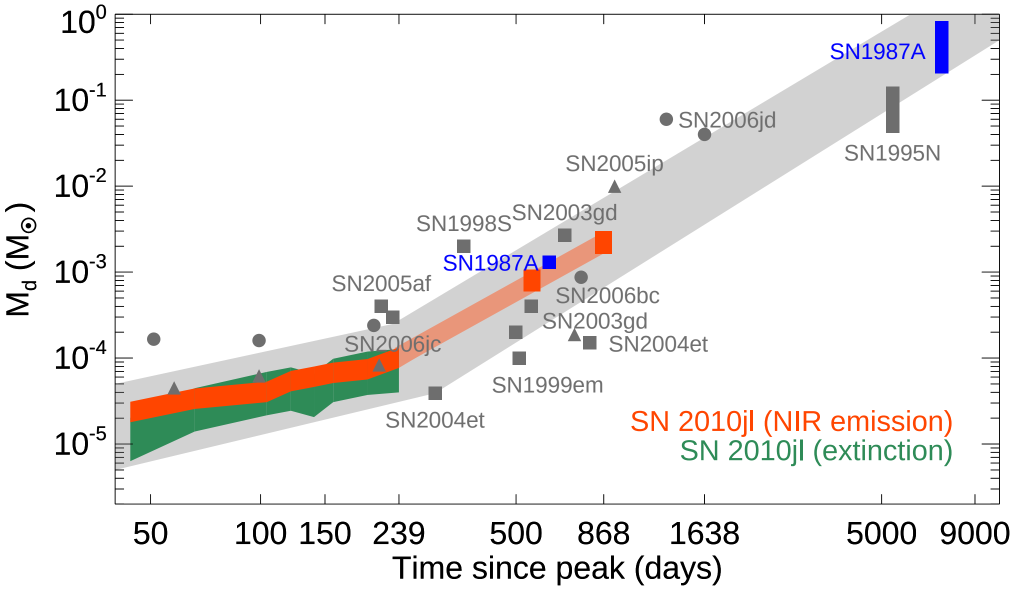
10^0
10^{-1}
10^{-2}
10^{-3}
10^{-4}
10^{-5}
M_d ($M_\odot$)
SN1987A
SN2006jd
SN1995N
SN2005ip
SN1998S
SN2003gd
SN1987A
SN2005af
SN2006bc
SN2003gd
SN2006jc
SN2004et
SN1999em
SN2004et
SN 2010jl (NIR emission)
SN 2010jl (extinction)
50
100
150
239
500
868
1638
5000
9000
Time since peak (days)